



Published in final edited form as:

Nat Immunol. 2013 November ; 14(11): 1183–1189. doi:10.1038/ni.2732.

A DNA break– and phosphorylation-dependent positive feedback loop promotes immunoglobulin class-switch recombination

Bao Q Vuong¹, Kayleigh Herrick-Reynolds^{#1}, Bharat Vaidyanathan^{#1,2}, Joseph N Pucella^{#1}, Anna J Ucher³, Nina M Donghia⁴, Xiwen Gu⁵, Laura Nicolas¹, Urszula Nowak^{1,2}, Numa Rahman¹, Matthew P Strout⁵, Kevin D Mills⁴, Janet Stavnezer³, and Jayanta Chaudhuri^{1,2}

¹Immunology Program, Memorial Sloan-Kettering Cancer Center, Gerstner Sloan-Kettering Graduate School, New York, New York, USA

²Immunology and Microbial Pathogenesis Program, Weill-Cornell Graduate School of Medical Sciences, New York, New York, USA

³Department of Microbiology & Physiological Systems, University of Massachusetts Medical School, Worcester, Massachusetts, USA

⁴The Jackson Laboratory, Bar Harbor, Maine, USA

⁵Yale Cancer Center, Yale University School of Medicine, New Haven, Connecticut, USA

These authors contributed equally to this work.

Abstract

The ability of activation-induced cytidine deaminase (AID) to efficiently mediate class-switch recombination (CSR) is dependent on its phosphorylation at Ser38; however, the trigger that induces AID phosphorylation and the mechanism by which phosphorylated AID drives CSR have not been elucidated. Here we found that phosphorylation of AID at Ser38 was induced by DNA breaks. Conversely, in the absence of AID phosphorylation, DNA breaks were not efficiently generated at switch (S) regions in the immunoglobulin heavy-chain locus (*Igh*), consistent with a failure of AID to interact with the endonuclease APE1. Additionally, deficiency in the DNA-damage sensor ATM impaired the phosphorylation of AID at Ser38 and the interaction of AID with APE1. Our results identify a positive feedback loop for the amplification of DNA breaks at S regions through the phosphorylation- and ATM-dependent interaction of AID with APE1.

© 2013 Nature America, Inc. All rights reserved.

Correspondence should be addressed to J.C. (chaudhuj@mskcc.org) or J.S. (janet.stavnezer@umassmed.edu).

Note: Any Supplementary Information and Source Data files are available in the online version of the paper.

AUTHOR CONTRIBUTIONS

B.Q.V. and J.C. conceived of the study and wrote the paper; B.Q.V., K.H.-R., B.V., J.N.P. and U.N. did the ChIP experiments; B.Q.V., K.H.-R. and B.V. did the coimmunoprecipitation and *in vitro* binding experiments; A.J.U. and J.S. did the LM-PCR experiment and bred the *Apex1*^{+/-}*Apex2*^{-/-} mice; N.M.D. and K.D.M. did the immuno-FISH; X.G. and M.P.S. bred the *Ung*^{-/-}*Msh2*^{-/-} mice; and N.R., B.Q.V., K.H.-R. and L.N. bred and analyzed the *Aicda*^{-/-}, *Atm*^{-/-} and *Aicda*^{S38A/S38A} mice.

COMPETING FINANCIAL INTERESTS

The authors declare no competing financial interests.

Class-switch recombination (CSR) is a DNA deletional-recombination event in the immunoglobulin heavy-chain locus (*Igh*) of mature B cells whereby exons encoding the default constant μ -chain (C_{μ}) are excised to juxtapose a new C-gene segment (for example, C_{γ} , C_{ϵ} or C_{α}) downstream of the rearranged variable (V) region to produce immunoglobulin G (IgG), IgE or IgA¹. CSR proceeds through the generation of DNA double-stranded breaks (DSBs) in switch (S) sequences that precede each constant heavy-chain (C_H) gene and is completed by end-joining between donor and acceptor S regions. CSR is a multistep reaction that requires transcription through S regions, the DNA cytidine deaminase AID^{2,3} and the participation of several general DNA-repair pathways, including base-excision repair (BER), mismatch repair (MMR) and nonhomologous end-joining (NHEJ)¹.

Current models posit that CSR is initiated by AID-mediated deamination of deoxycytidine residues to deoxyuridine residues in transcribed S regions¹. The BER enzyme UNG (uracil DNA glycosylase) excises the uracil base to create an abasic site^{4,5}. The phosphodiester bond at the abasic site is probably cleaved by the apurinic-apyrimidinic endonucleases APE1 and APE2 to generate a single-stranded break (SSB)^{6,7}. Two closely spaced SSBs on opposite strands constitute a DSB, an obligate intermediate step of CSR⁸⁻¹¹. Conversion of widely separated SSBs into a DSB requires further processing by components of the MMR pathway¹. Once formed, DSBs between donor and acceptor S regions are ligated by DNA end-joining proteins. Both canonical NHEJ, which ligates DNA with little or no homology, and a poorly defined alternative NHEJ process, which requires ‘microhomology’ of DNA ends for ligation, participate in the end-joining phase of CSR¹. Mutations in genes encoding components of the MMR, BER and NHEJ pathways, including UNG, Msh2 and APE1-APE2, result in less CSR, which provides genetic evidence for this proposed model of CSR¹.

In addition to undergoing CSR, mature B cells undergo another AID-dependent gene diversification reaction, somatic hypermutation (SHM), whereby untemplated mutations are introduced into the V region to generate high-affinity immunoglobulins¹². Like CSR, SHM also proceeds through the processing of deaminated residues by components of the BER and MMR pathways but does not require DNA breaks. Thus, in B cells undergoing an immune response, the immunoglobulin V-region genes and S-region DNA serve as the physiological targets of AID. However, AID can induce lesions at several non-immunoglobulin genes, and such aberrant AID activity generates the mutations in and translocations of oncogenes that are responsible for the ontogeny of mature B cell lymphomas¹³. Therefore, AID expression is restricted by transcription and the stability of its mRNA, while its activity is regulated by intracellular localization, interaction with proteins (such as Spt5, RNA exosome subunits, 14-3-3 proteins and PTBP2) that actively recruit it to the *Igh* locus, the immunoglobulin κ -chain locus (*Igk*) and the immunoglobulin λ -chain locus (*Igl*), and phosphorylation at multiple residues¹⁴.

Phosphorylation of AID at Ser38 has emerged as a major mechanism by which CSR is regulated. Mice with a knock-in mutation of the gene encoding AID (*Aicda*) that results in replacement of the serine at position 38 with alanine (*Aicda*^{S38A/S38A} mice) have severe defects in CSR^{15,16}. Ser38 lies within a consensus site for phosphorylation by protein kinase A (PKA)¹⁶⁻¹⁸, and hypomorphic mutations in the gene encoding PKA reduce the

phosphorylation of AID at Ser38 and substantially impair CSR¹⁹. Additionally, PKA associates with S regions during CSR, which suggests that PKA is recruited to S regions to induce phosphorylation of AID at Ser38, which consequently activates the CSR reaction cascade¹⁹. The concerted recruitment of PKA and AID to S regions provides a mechanism whereby multiple molecules of AID can be synchronously activated to introduce a high density of DNA breaks in S regions, which are required for CSR¹⁹. While compelling, such a regulatory process would require an as-yet-undescribed trigger that would induce the phosphorylation of AID molecules bound to S regions. In this study, we identified a positive feedback loop wherein DNA breaks induced the phosphorylation of AID at Ser38 and subsequent binding of APE1, which accentuated the formation of DNA breaks at S regions and amplification of AID phosphorylation through a pathway dependent on the DNA-damage sensor ATM.

RESULTS

Deaminase-inactive S region-bound AID is unphosphorylated

AID phosphorylated at Ser38 (p-Ser38-AID; also called ‘phosphorylated AID’ here) acquires the ability to interact with replication protein A (RPA)^{17,20}. RPA participates in many aspects of DNA metabolism, including DNA replication, the DNA-damage checkpoint and all major forms of DNA repair (such as BER and DSB repair). In B cells undergoing CSR, RPA binds to transcribed S regions in a manner dependent on p-Ser38-AID¹⁹⁻²². We initially sought to determine if the interaction of RPA with p-Ser38-AID was sufficient for RPA to stably bind S regions or if the DNA-binding ability of RPA was stabilized by AID-dependent DNA deamination, which would be consistent with the well-defined ability of RPA to bind single-stranded DNA during DNA repair²³.

We used a previously characterized catalytically inactive AID mutant, AID(DM), that has two mutations (encoding the substitutions H56R and E58Q) in the deaminase domain of AID^{24,25}. We introduced AID(DM) into AID-deficient splenic B cells through retroviral transduction. As controls, we reconstituted AID-deficient B cells with empty vector or with vector encoding wild-type AID (AID(WT)) or the phosphorylation-site mutant AID(S38A). We stimulated the transduced B cells with lipopolysaccharide (LPS) and interleukin 4 (IL-4) to induce CSR to IgG1. As expected, AID(S38A) was approximately 15–25% as active as AID(WT) in restoring CSR, and AID(DM) did not restore CSR frequency over what we observed for the cells transduced with the empty vector control (Supplementary Fig. 1a). Immunoblot analysis showed that the different AID proteins had equivalent expression in transduced B cells (Supplementary Fig. 1b). Furthermore, AID(DM) retained the ability to bind to RPA in a PKA-dependent fashion (Supplementary Fig. 1c,d). Thus, AID(DM) was equivalent to AID(WT) in its ability to be a PKA substrate and to interact with RPA *in vitro*.

To assess the binding of RPA to S regions in the absence of DNA deamination, we used chromatin immunoprecipitation (ChIP) with antibody to RPA (anti-RPA) to precipitate DNA-protein complexes from splenic B cells expressing various forms of AID and stimulated with LPS plus IL-4 (Fig. 1). For this ChIP we also used anti-AID, anti-histone H3 as a positive control, and nonspecific IgG to compensate for background immunoprecipitation. We analyzed the DNA-protein complexes recovered after ChIP for the

recombining S regions S_{μ} and $S_{\gamma 1}$ (Fig. 1) and for sequences not generally targeted by AID in B cells stimulated to undergo CSR ($C_{\gamma 1}$ and $Trp53$) (Supplementary Fig. 2). As reported before^{19,21}, we readily detected RPA bound to S regions in a p-Ser38-AID-dependent manner. In contrast, in cells expressing AID(DM), the binding of RPA to S regions was substantially reduced, even though AID(DM) was as competent as AID(WT) in binding both S_{μ} and $S_{\gamma 1}$ (Fig. 1). Overall, these results demonstrated that in B cells expressing catalytically inactive AID, RPA binding to activated S regions was markedly impaired.

The defect in the binding of RPA to S-region DNA in cells expressing AID(DM) was similar to that observed in AID(S38A) cells (Fig. 1). That observation prompted us to investigate whether AID(DM) bound to DNA was phosphorylated at Ser38. For this, we did ChIP with an antibody specific for p-Ser38-AID¹⁹. The antibody detected AID(WT) or AID(DM) phosphorylated *in vitro* with PKA but did not detect AID(S38A) (Supplementary Fig. 3). We observed that in contrast to AID(WT), AID(DM) was poorly phosphorylated when bound to transcribed S regions (Fig. 1). The binding of PKA to S regions was similar for cells expressing AID(WT) and those expressing AID(DM) (Supplementary Fig. 4), which indicated that the diminished phosphorylation of AID(DM) was not due to altered binding of PKA to S regions. Thus, even though AID(DM) was a PKA substrate *in vitro*, this mutant AID protein was not efficiently phosphorylated when bound to S regions *in vivo*. These data suggested that the phosphorylation of AID at Ser38 and subsequent recruitment of RPA to S regions was dependent on either DNA deamination or the processing of deaminated residues into DNA breaks.

DNA breaks induce phosphorylation of AID bound to S regions

To determine whether DNA breaks at S regions were able to induce phosphorylation of AID, we investigated whether artificially generated DSBs in cells expressing AID(DM) were able to promote its phosphorylation. We retrovirally transduced AID-deficient splenic B cells with AID(WT), AID(DM), AID(S38A) or the empty vector control, activated them as described above, treated them with 10 Gy of ionizing radiation and then analyzed them by ChIP (Fig. 2a). Ionizing radiation induced the formation of genome-wide DSBs, which was evident in the AID-independent binding of RPA to all genomic sequences analyzed (S_{μ} , $S_{\gamma 1}$, $C_{\gamma 1}$ and $Trp53$; Fig. 2a and Supplementary Fig. 2). Treatment with ionizing radiation did not affect the binding of AID proteins to S regions or the phosphorylation of AID(WT) bound to S regions (Figs. 1 and 2a). However, in contrast to what we observed for cells that were not irradiated (Fig. 1), ionizing radiation markedly enhanced the phosphorylation of AID(DM) bound to S-region DNA (Fig. 2a). The amount of p-Ser38-AID(DM) bound to S_{μ} and $S_{\gamma 1}$ was similar to that observed for p-Ser38-AID(WT). We also observed the ionizing radiation-dependent increase in the phosphorylation of AID(DM) at Ser38 and the subsequent binding of RPA in an analogous assay in which we immunoprecipitated p-Ser38-AID from lysates of AID-deficient ($Aicda^{-/-}$) B cells retrovirally infected as described above and analyzed immunoprecipitates by immunoblot with anti-AID or anti-RPA (Fig. 2b). Thus, the induction of phosphorylation at Ser38 on deaminase-inactive AID by ionizing radiation treatment suggested that the artificial induction of DNA breaks enhanced the phosphorylation of AID at Ser38.

In B cells undergoing CSR, the initial DNA lesion induced by AID is in the form of DNA deamination. Subsequent conversion of the deaminated residues into DSBs requires proteins involved in BER and MMR^{5,26,27}. To directly determine whether DNA deamination or DSBs induced the phosphorylation of AID, we studied mice deficient in UNG and Msh2 (*Ung*^{-/-}*Msh2*^{-/-} mice)⁵. In *Ung*^{-/-}*Msh2*^{-/-} B cells, AID can induce the deamination of S-region DNA²⁸ but the deaminated residues are not converted into DNA breaks^{27,29}. Splenic B cells from *Ung*^{-/-}*Msh2*^{-/-} mice stimulated *ex vivo* with LPS plus IL-4 do not undergo CSR to any appreciable frequency⁵. ChIP experiments showed that the abundance of AID at recombining S regions was equivalent in wild-type, *Aicda*^{S38A/S38A} and *Ung*^{-/-}*Msh2*^{-/-} B cells; however, the amount of p-Ser38-AID and, consequently, the abundance of RPA at S regions in *Ung*^{-/-}*Msh2*^{-/-} B cells was significantly lower than that in wild-type B cells and was similar to that in *Aicda*^{S38A/S38A} B cells (Fig. 2c). These results suggested that lesions in the form of DNA deamination were not sufficient to induce the phosphorylation of AID bound to activated S regions; instead, conversion of the deaminated residues into DNA breaks was required for phosphorylation of AID.

To further demonstrate that phosphorylation of AID was induced by DNA breaks at S regions, we assessed AID phosphorylation in B cells heterozygous for deficiency in APE1 and homozygous for deficiency in APE2 (*Apex1*^{+/-}*Apex2*^{-/-}). APE1 is the main apurinicapyrimidinic endonuclease in mammalian cells, while APE2 has 3'-to-5' exonuclease activity with weak endonuclease activity at apurinic-apyrimidinic sites. APE1 is generally believed to cleave the phosphodiester backbone at the apurinic-apyrimidinic sites generated after AID and UNG act at S regions^{4,6,7}. *Apex1*-null mutations in mice lead to embryonic death³⁰; however, *Apex1*^{+/-}*Apex2*^{-/-} mice were viable and had impaired CSR, probably because of defects in DNA-break formation at S regions^{6,31} (Fig. 2d). Consistent with the ability of DNA breaks to stimulate the phosphorylation of AID, we observed a lower abundance of p-Ser38-AID at transcribed S regions in *Apex1*^{+/-}*Apex2*^{-/-} B cells than in wild-type cells (Fig. 2e and Supplementary Fig. 5). Overall, these data suggested that DNA breaks generated at S regions induced phosphorylation of AID at Ser38.

Phosphorylation of AID bound to S regions induces DSB formation

The increased phosphorylation of AID after the formation of DSBs at S regions suggested the existence of a positive feedback loop that amplifies AID phosphorylation and AID-dependent DNA-break formation whereby a few DNA breaks generated by AID in a phosphorylation-independent manner induce AID phosphorylation, which in turn leads to additional breaks. If such a positive feedback loop exists, then *Aicda*^{S38A/S38A} B cells should display fewer DNA breaks at recombining S regions. To assess that possibility, we stimulated splenic B cells from wild-type, *Aicda*^{-/-} or *Aicda*^{S38A/S38A} mice with LPS alone, LPS plus IL-4, or LPS plus interferon- γ , isolated genomic DNA from the cells and detected DSBs at S _{μ} by ligation-mediated PCR (LM-PCR). This assay has been used to demonstrate the presence of DSBs in S regions in stimulated splenic B cells and to assess the requirements for AID, UNG and APE1-APE2 in the formation of such DSBs^{6,11,27,29,32}. We detected significantly fewer DSBs at S _{μ} in *Aicda*^{S38A/S38A} B cells than in wild-type B cells under all three experimental conditions, and the abundance of DSBs in *Aicda*^{S38A/S38A} B cells was similar to that in *Aicda*^{-/-} B cells (Fig. 3 and Supplementary Fig. 6). Furthermore,

treatment of the genomic DNA with T4 DNA polymerase before linker ligation, which blunts DSBs at staggered overhangs, also resulted in similarly less DSB formation at S_{μ} in *Aicda*^{S38A/S38A} B cells than in wild-type B cells (Fig. 3 and Supplementary Fig. 6).

In a complementary assay, we analyzed colocalization of the *Igh* locus with phosphorylated γ -H2AX foci, a marker for DSBs, by combined immunofluorescence labeling and fluorescent *in situ* hybridization (immuno-FISH), which has been used extensively as a measure of AID-initiated DSBs at the *Igh* locus^{10,33}. We stimulated splenic B cells with anti-CD40 plus IL-4 and evaluated the colocalization of γ -H2AX with *Igh* FISH signals (Fig. 4a) by determining the frequency of cells with at least one colocalization event (Fig. 4b). Consistent with the LM-PCR data, significantly fewer *Aicda*^{S38A/S38A} B cells than wild-type cells had γ -H2AX foci that colocalized with the *Igh* locus (Fig. 4 and Supplementary Fig. 7). Thus, both the LM-PCR and immuno-FISH results suggested that *Aicda*^{S38A/S38A} B cells were impaired in their ability to introduce DSBs at S regions; these results also provided further evidence of the positive feedback loop of AID phosphorylation and DNA-break formation during CSR.

We next investigated the mechanism by which the phosphorylation of AID induced DNA-break formation. On the basis of the results described above for the positive feedback mechanism of AID phosphorylation and DNA-break formation at recombining S regions and published observations showing that phosphorylation of AID at Ser38 does not affect the binding of AID to S regions *in vivo* or DNA deamination *in vitro*¹⁹, we reasoned that phosphorylation of AID might enhance its ability to interact with APE1. To test that possibility, we investigated whether phosphorylated AID was able to interact with APE1 in lysates of *Aicda*^{-/-} B cells retrovirally reconstituted with hemagglutinin (HA)-Flag-tagged AID constructs or the empty vector control. Proteins immunoprecipitated with anti-HA from cells expressing HA-Flag-tagged AID(WT) were enriched for APE1 in the presence or absence of ionizing radiation (Fig. 5a). The interaction of wild-type AID with APE1 was dependent on Ser38 and PKA, as the HA-Flag-AID(S38A) mutant did not immunoprecipitate together with APE1 (Fig. 5a), and AID(WT) ectopically expressed in human embryonic kidney (293T) cells did not interact with APE1 in the absence of phosphorylation by PKA *in vitro* (Supplementary Fig. 8). With lysates of *Aicda*^{-/-} B cells retrovirally reconstituted with untagged AID proteins, we confirmed the Ser38-dependent interaction of AID(WT) with APE1 and RPA in samples immunoprecipitated with anti-APE1 (Fig. 5b) or antibody to p-Ser38-AID (Fig. 5c). APE1 did not interact with RPA in the absence of AID (Fig. 5b), nor did recombinant, phosphorylated AID interact with APE1 in the presence of purified RPA (Supplementary Fig. 9).

Consistent with the results obtained by ChIP, which showed that AID(DM) was phosphorylated in the presence of ionizing radiation, AID(DM) interacted with APE1 only after treatment with ionizing radiation (Fig. 5a-c). Similarly, in *Ung*^{-/-}*Msh2*^{-/-} B cells, which did not have DSBs in S regions, the AID-APE1 interaction was significantly augmented after treatment with ionizing radiation (Fig. 5d). Treatment of cell extracts with DNase I before immunoprecipitation did not abrogate the AID-APE1 interaction (Fig. 5e), which suggested that the association was not dependent on DNase I-sensitive DNA. These

results suggested that phosphorylation of AID at Ser38 augmented DNA-break formation by recruiting APE1 to S-region DNA.

ATM promotes AID phosphorylation and APE1 binding

We next investigated the mechanism by which DNA breaks at S regions induced the phosphorylation of AID at Ser38. ATM is rapidly activated in response to DSBs and serves a critical role in the cellular response to DSBs by phosphorylating DNA-repair proteins, such as CHK2 and NBS1 (ref. 34). CSR is significantly impaired in ATM-deficient B cells, and ATM has been proposed to function in the synapsis of recombining S regions^{35,36}. We therefore determined whether ATM was able to activate PKA-mediated phosphorylation of AID in response to DNA breaks. ChIP analysis showed that *Atm*^{-/-} B cells had a significant reduction in the amount of p-Ser38-AID at S_μ and S_γ1 (Fig. 6a and Supplementary Fig. 10). Consistent with the possibility of a positive feedback loop for DSB formation and AID phosphorylation, we readily detected the interaction of AID with APE1 in wild-type B cells, but it was significantly attenuated in *Atm*^{-/-} B cells (Fig. 6b). The impaired phosphorylation of AID bound to S regions and reduced interaction of AID with APE1 in *Atm*^{-/-} B cells was not abolished as it was in *Aicda*^{-/-} and *Aicda*^{S38A/S38A} B cells (Fig. 6), which suggested that a compensatory kinase (for example, ATM-kinase related (ATR)) may act in the absence of ATM. Together these results identified an ATM-dependent pathway required for the efficient phosphorylation of AID bound to S regions activated for recombination and for the interaction of AID with APE1.

DISCUSSION

Given the interdependence between AID phosphorylation and DNA-break formation, we propose a model in which unphosphorylated AID bound to S regions can induce low frequencies of DNA deamination that can be resolved by the BER or MMR pathway into a DSB. That process promotes phosphorylation of AID through activation of the S region-bound catalytic subunit of PKA¹⁹ via an ATM-dependent pathway. The phosphorylation of AID leads to the increased formation of DNA breaks at S regions through the recruitment of APE1. That in turn induces additional AID phosphorylation and amplifies DNA-break formation to generate the number of DSBs sufficient for wild-type frequencies of CSR. The positive feedback loop for amplifying DNA breaks elicits at least three related questions.

First, what advantage does a positive feedback loop provide to the basic process of CSR? We favor the proposal that CSR requires a high density of DSBs to promote end-joining between DSBs generated at two different distal S regions. Thus, even though AID and PKA assemble at S regions¹⁹, AID is not efficiently phosphorylated until a DNA break is generated. Once a DNA break is formed, the rapid activation of AID phosphorylation and DSB formation results in the synchronous activation of many molecules of AID bound to an S region. The high density of DSBs in S regions thus generates many broken DNA ends that promote the ligation of distal DSBs, which subverts normal DNA repair. When AID phosphorylation is blocked, as in B cells expressing AID(S38A), or diminished, as in B cells with mutant hypomorphic PKA, the low density of DSBs induced at individual S regions could be resolved as inefficient CSR or as intra-S-region joining in nonproductive

recombination¹⁹. The proposed positive feedback loop requires coordinated recruitment of both AID and PKA to recombining S regions, which may be a regulatory mechanism for limiting AID activity at non-immunoglobulin genes. While AID can bind and deaminate several non-immunoglobulin genes^{21,37}, very few of those lesions would be converted into DSBs in the absence of AID phosphorylation. Thus, the two-tiered mode of AID activation (recruitment to S regions and subsequent phosphorylation by PKA) provides a mechanism with which to generate a high density of DSBs specifically at *Igh* S regions during CSR while restricting DSB formation at non-immunoglobulin sites. In this context, we speculate that SHM, which does not proceed through DSB intermediates, has no requirement for that positive feedback loop, as low numbers of AID-instigated lesions at V-region genes could be resolved as mutations through engagement of the BER or MMR pathway⁴. However, phosphorylation of AID at Ser38 is still required for it to interact with RPA, which in turn facilitates the binding of AID to V-region genes during SHM²⁰.

The second question that arises is the mechanism by which the phosphorylation of AID induces DNA-break formation. Here we found that the interaction of AID with APE1 was dependent on PKA and Ser38. APE1 has been proposed to participate in CSR by cleaving phosphodiester bonds at abasic sites generated after the combined activities of AID and UNG, the latter of which is recruited to S regions by the carboxyl terminus of AID^{4,6,7,38}. While APE1 could passively access the abasic sites generated through basal AID activity, APE1 may be actively recruited to the sites of AID-induced deamination through its interaction with p-Ser38–AID, which would facilitate the rapid and efficient conversion of abasic sites into DNA breaks. The phosphorylation-dependent binding of AID to APE1 was not mediated through RPA, as *in vitro* binding experiments with purified recombinant proteins showed that p-Ser38–AID did not interact with APE1 in the presence of RPA. In addition, APE1 did not bind RPA in the absence of AID. These data suggested that AID bridges the interaction between APE1 and RPA and that the binding of APE1 to AID requires an as-yet-unidentified cofactor. Transcription through S regions during CSR may generate or expose nucleic acid substrates and/or binding sites on AID to mediate the interaction of AID with APE1. Alternatively, other proteins known to interact with AID, such as PTBP2, Spt5, 14-3-3 or the RNA exosome, may function to recruit that protein complex to the transcribed S regions¹⁴.

Finally, a positive feedback loop of DNA break–induced phosphorylation of AID at Ser38 would suggest that the activity of the AID kinase PKA may be regulated by DSB signaling pathways¹⁹. The PKA-C α catalytic subunit has a Ser-Gln sequence at its amino terminus (Ser35), which is a consensus site for phosphorylation by ATM and ATR. We speculate that Ser35 of PKA-C α could be phosphorylated by ATM or ATR, leading to an enhanced ability to phosphorylate AID at Ser38. Alternatively, ATM or ATR may initiate a signaling cascade to locally increase cAMP concentrations at S regions to activate PKA and facilitate the phosphorylation of AID at Ser38. Consistent with both of those proposals, PKA has been linked to the DNA-damage response to ionizing radiation³⁹, and ATR has been proposed to regulate the phosphorylation of PKA substrates in response to DNA damage⁴⁰.

In summary, we have identified a role for ATM in promoting the phosphorylation-dependent interaction between AID and APE1, which ensures that CSR proceeds through the canonical

BER pathway that is the main effector of CSR⁵. We propose that ATM-deficient cells do not actively engage BER proteins, especially APE1, to process the G:U mismatch; instead, the MMR pathway, which has a less potent role in CSR⁵, converts the deaminated residues into DNA breaks, which promotes the phosphorylation of AID through an ATR-dependent reaction. In this context, ATR has been shown to interact with the MMR proteins Msh2 and Msh6, which bind to the G:U mismatch⁴¹. That hypothesis is consistent with our observation that the diminished phosphorylation of AID at S regions in ATM-deficient cells was not as severe as the decrease in the AID-APE1 interaction. Furthermore, ATM deficiency also impairs interactions between S regions^{35,36} and, when combined with a failure to enforce cell-cycle checkpoints at the G1-S transition, leads to the persistence of DSBs that can participate in aberrant chromosomal translocations⁴². Therefore, the AID-APE1-DSB-ATM positive feedback loop generates a threshold number of DNA breaks precisely within transcribed S regions and promotes the joining of distal recombining S regions to permit successful CSR while suppressing oncogenic translocations.

ONLINE METHODS

Plasmids, mice, antibodies, and reagents

The empty vector (pMIG) and pCL-Eco constructs used in retroviral infections have been described¹⁹. The HA-Flag-tagged forms of AID were cloned by PCR amplification with primers containing sequence encoding HA and Flag upstream of the ATG start codon of mouse *Aicda*. Constructs encoding AID(S38A) and AID(DM) were cloned with a Quickchange site-directed mutagenesis kit (Stratagene). The generation of *Aicda*^{-/-}, *Aicda*^{S38A/S38A}, *Ung*^{-/-}*Msh2*^{-/-}, *Apex1*^{+/-}*Apex2*^{-/-} and *Atm*^{-/-} mice has been described^{2,5,6,15,43}. Wild-type control BALB/c mice were from The Jackson Laboratories. Antibodies for CHIP, immunoblot analysis and flow cytometry were as follows: anti-AID and antibody to p-Ser38-AID have been described^{19,24}; anti-RPA (NA19L-100UG; EMD), anti-H3 (ab1791; Abcam), anti-APE1 (AF1044; R&D Systems), anti-HA (11867423001; Roche), allophycocyanin-conjugated anti-mouse IgG1 (550874; BD Pharmingen) and rabbit IgG (I5006; Sigma). Antibodies for immunoprecipitation were as follows: antibody to p-Ser38-AID was conjugated to agarose beads with an AminoLink Plus Immobilization Kit (44894; Pierce) by the Memorial Sloan-Kettering Monoclonal Antibody Core Facility; anti-HA conjugated to agarose (26181; Pierce); and anti-APE1 (AF1044; R&D Systems). H89 (protein kinase inhibitor; B1427) and NaF (201154) were from Sigma.

Purification, stimulation and retroviral infection of B cells

The purification of naive, mature B cells, retroviral infection and stimulation conditions to induce CSR have been described¹⁹. For CSR experiments, cells were stimulated in medium containing LPS and IL-4 on day 0 and were supplemented with an equal volume of medium supplemented with LPS (25 µg/ml) plus IL-4 (12.5 ng/ml) on day 2, then were analyzed for CSR by flow cytometry on day 4. For irradiation experiments, cells were harvested 24 h after the second infection (72 h after the initial stimulation) and were left untreated or were treated with 10 Gy of ionizing radiation from a ¹³⁷Cs source. The cells were incubated for 10 min at 37 °C before they were fixed in 1% formaldehyde and processed for ChIP.

Immunoprecipitation

B cells stimulated for 72 h with LPS plus IL-4 were harvested and resuspended in NP-40 lysis buffer (0.5% Nonidet P-40, 50 mM Tris, pH 7.5, 100 mM NaCl, 0.1 mM EDTA, 20 μ M H89 and 10 mM NaF). For retroviral infections, cells were harvested 24 h after the second infection (72 h after the initial stimulation) and either treated or untreated with 10 Gy of ionizing radiation from a Cesium-137 source. The infected (irradiated and unirradiated) cells were incubated for 10 min at 37 °C before they were harvested, washed in PBS and resuspended in NP-40 lysis buffer. The lysates were incubated for 30 min at 4 °C and then were sonicated with a Branson digital sonifier (10% amplitude, 10 s pulses, three times). The lysates were spun at 20,800g for 10 min at 4 °C. The supernatants were removed and assayed for protein concentration by the Bradford assay (Bio-Rad). Lysates (500 μ g) were precleared for 1 h at 4 °C with agarose beads (IC19345280; VWR) for immunoprecipitation of p-Ser38-AID and HA and with protein A agarose beads (IP06-10ML; EMD) plus rabbit IgG (I5006; Sigma) for immunoprecipitation of AID and APE1. Lysates were immunoprecipitated for 2 h for immunoprecipitation of p-Ser38-AID and HA or 1 h with anti-AID or anti-APE1, followed by 1 h with protein A agarose beads. Immunoprecipitates were washed three times with NP-40 lysis buffer and analyzed by immunoblot.

LM-PCR and ChIP

Cells used for LM-PCR were cultured as described⁴⁴, except LPS was used at a concentration of 25 μ g/ml, and dextran-coupled anti-IgD (10 ng/ml; 11.26c; FinaBio) was added to all cultures. LM-PCR and calculation of the relative quantity of DSBs were done as described^{27,31}. ChIP experiments and calculations of ChIP (relative units) were done as described¹⁹.

ChIP primers

ChIP DNA was analyzed by quantitative PCR with iQ SYBR Green Supermix (Bio-Rad) for S_{μ} , *Trp53* and $C_{\gamma}1$. Primers to amplify S_{μ} were muSf (5'-TAGTAAGCGAGGCTCTAAAAAGCAT-3') and muSr (5'-AGAACAGTCCAGTGTAGGCAGTAGA-3'). Primers to amplify *Trp53* were p53for (5'-TATACTCAGAGCCGGCCT-3') and p53rev (5'-CAGCGTGGTGGTAACCTTAT-3'). Primers to amplify $C_{\gamma}1$ were Cg1.F2 (5'-GGATCTGCTGCCCAAATAACTC-3') and Cg1R (5'-GGATCCAGAG TTCCAGGTCCT-3'). For $S_{\gamma}1$, a Taqman quantitative PCR assay was used in conjunction with FastStart Universal Probe Master Mix (Roche). The primers used to amplify $S_{\gamma}1$ were Sg1.f4 (5'-GCATTGGGATTAGAGTAACTAAGGG-3'), Sg1.r4 (5'-GCTTGCACTTTCTCTACTTGTC-3') and Sg1. tmp1 (5'-56-FAM-CCTCCTTCAATCCAGGGTTGCTTCT-3BHQ_1-3', where the 5' end of the oligonucleotide is conjugated to 6-carboxyfluorescein (56-FAM) and the 3' end is conjugated to Black Hole Quencher-1 (3BHQ_1)).

Immuno-FISH

Immuno-FISH was done as described³³. Cells were allowed to adhere to coverslips coated with poly-l-lysine (P8920-100ML; Sigma-Aldrich), were fixed with 4% paraformaldehyde

in PBS and were permeabilized with 0.5% Triton X-100 in PBS. Fixed cells were hybridized with an *Igh* probe (bacterial artificial chromosomal RP23-109B20) labeled with indocarbocyanine and were then stained with anti- γ -H2AX (A300-081A; Bethyl) followed by Alexa Fluor 488-conjugated anti-rabbit (A11034; Invitrogen). Samples were mounted with Vectashield containing DAPI counterstain (H-1200; Vector Laboratories), were imaged by epifluorescence wide-field microscopy with a Nikon 90i upright microscope and were analyzed with NIS Elements software.

RPA and APE1 precipitation assay

RPA was precipitated as described¹⁷. 293T cells transfected with empty vector (plasmid pMIG) expressing various AID variants were lysed in NP-40 lysis buffer. Lysates from untransfected cells were used as the source of RPA and APE1 in the binding assay. AID was immunoprecipitated from 500 μ g of the soluble lysate, the immunoprecipitates were washed with lysis buffer and then with PKA buffer (20 mM Tris, pH 7.5, 80 mM NaCl, 1 mM DTT, 10 mM MgCl₂, 1 mM ATP and 10 μ M cAMP) and equal volumes were placed into two separate tubes. The immunoprecipitates were incubated for 30 min at 30 °C with or without recombinant PKA (P6000S; NEB) in PKA buffer. The immunoprecipitates were washed with lysis buffer and then incubated with soluble NP-40 lysates of untransfected 293T cells (250 μ g). The complexes were washed and analyzed by immunoblot.

Recombinant RPA, APE1 and MBP-AID *in vitro* binding assay

Recombinant APE1 was purified as described⁴⁵. Recombinant human RPA (a gift from J. Hurwitz) was purified as described⁴⁶, except a MonoQ column (GE Healthcare) was used in place of a Q-Sepharose column in the final purification step. Constructs encoding AID(S38A) and AID(DM) were cloned with a Quickchange site-directed mutagenesis kit (Stratagene). Maltose-binding protein (MBP) and an MBP-AID fusion protein were purified and remained bound to amylose beads during the *in vitro* binding assay. Beads containing 15 μ g of MBP or MBP-AID were washed with PKA buffer. The beads were resuspended in PKA buffer and half was removed to control for the presence of PKA. Recombinant PKA (P6000S; NEB) or water was added and the beads were incubated for 1 h at 30 °C. The beads were pelleted and washed with PKA buffer followed by NP-40 lysis buffer. The beads were resuspended in NP-40 lysis buffer and then were incubated for 30 min at 4 °C with the purified, recombinant RPA and APE1. The beads were pelleted, washed twice with NP-40 lysis buffer and analyzed by immunoblot.

Statistical analysis

Unless otherwise noted, a paired, two-tailed Student's *t*-test was used for statistical analysis.

Supplementary Material

Refer to Web version on PubMed Central for supplementary material.

Acknowledgments

We thank J. Hurwitz (Memorial Sloan-Kettering Cancer Center) for recombinant human RPA; members of the Chaudhuri laboratory, D. Sant' Angelo and L. Denzin for critically reviewing the manuscript and for discussions

and suggestions; V. Bermudez and J. Hurwitz for help in purifying recombinant human RPA; J. Lange and S. Keeney (Memorial Sloan-Kettering Cancer Center) for *Atm*^{-/-} mice; and D.M. Wilson III (US National Institutes of Health) for the plasmid for expression of human APE1. Supported by the US National Institutes of Health (RO1AI23283 and R21 AI099908 to J.S., 5 R01 CA138646-04 to K.D.M. and 1RO1AI072194 to J.C.) and the Starr Cancer Consortium (I4-A447 to J.C.).

References

1. Stavnezer J, Guikema JE, Schrader CE. Mechanism and regulation of class switch recombination. *Annu. Rev. Immunol.* 2008; 26:261–292. [PubMed: 18370922]
2. Muramatsu M, et al. Class switch recombination and hypermutation require activation-induced cytidine deaminase (AID), a potential RNA editing enzyme. *Cell.* 2000; 102:553–563. [PubMed: 11007474]
3. Revy P, et al. Activation-induced cytidine deaminase (AID) deficiency causes the autosomal recessive form of the Hyper-IgM syndrome (HIGM2). *Cell.* 2000; 102:565–575. [PubMed: 11007475]
4. Petersen-Mahrt SK, Harris RS, Neuberger MS. AID mutates *E. coli* suggesting a DNA deamination mechanism for antibody diversification. *Nature.* 2002; 418:99–103. [PubMed: 12097915]
5. Rada C, Di Noia JM, Neuberger MS. Mismatch recognition and uracil excision provide complementary paths to both Ig switching and the A/T-focused phase of somatic mutation. *Mol. Cell.* 2004; 16:163–171. [PubMed: 15494304]
6. Guikema JE, et al. APE1- and APE2-dependent DNA breaks in immunoglobulin class switch recombination. *J. Exp. Med.* 2007; 204:3017–3026. [PubMed: 18025127]
7. Masani S, Han L, Yu K. Apurinic/aprimidinic endonuclease 1 is the essential nuclease during immunoglobulin class switch recombination. *Mol. Cell. Biol.* 2013; 33:1468–1473. [PubMed: 23382073]
8. Iwasato T, Arakawa H, Shimizu A, Honjo T, Yamagishi H. Biased distribution of recombination sites within S regions upon immunoglobulin class switch recombination induced by transforming growth factor β and lipopolysaccharide. *J. Exp. Med.* 1992; 175:1539–1546. [PubMed: 1588279]
9. Matsuoka M, Yoshida K, Maeda T, Usuda S, Sakano H. Switch circular DNA formed in cytokine-treated mouse splenocytes: evidence for intramolecular DNA deletion in immunoglobulin class switching. *Cell.* 1990; 62:135–142. [PubMed: 2114219]
10. Petersen S, et al. AID is required to initiate Nbs1/ γ -H2AX focus formation and mutations at sites of class switching. *Nature.* 2001; 414:660–665. [PubMed: 11740565]
11. Wuerffel RA, Du J, Thompson RJ, Kenter AL. Ig S γ 3 DNA-specific double strand breaks are induced in mitogen-activated B cells and are implicated in switch recombination. *J. Immunol.* 1997; 159:4139–4144. [PubMed: 9379005]
12. Papavasiliou FN, Schatz DG. Somatic hypermutation of immunoglobulin genes: merging mechanisms for genetic diversity. *Cell.* 2002; 109:S35–S44. [PubMed: 11983151]
13. Daniel JA, Nussenzweig A. The AID-induced DNA damage response in chromatin. *Mol. Cell.* 2013; 50:309–321. [PubMed: 23664375]
14. Vuong BQ, Chaudhuri J. Combinatorial mechanisms regulating AID-dependent DNA deamination: Interacting proteins and post-translational modifications. *Semin. Immunol.* 2012; 24:264–272. [PubMed: 22771392]
15. Cheng HL, et al. Integrity of the AID serine-38 phosphorylation site is critical for class switch recombination and somatic hypermutation in mice. *Proc. Natl. Acad. Sci. USA.* 2009; 106:2717–2722. [PubMed: 19196992]
16. McBride KM, et al. Regulation of class switch recombination and somatic mutation by AID phosphorylation. *J. Exp. Med.* 2008; 205:2585–2594. [PubMed: 18838546]
17. Basu U, et al. The AID antibody diversification enzyme is regulated by protein kinase A phosphorylation. *Nature.* 2005; 438:508–511. [PubMed: 16251902]
18. Pasqualucci L, Kitaura Y, Gu H, Dalla-Favera R. PKA-mediated phosphorylation regulates the function of activation-induced deaminase (AID) in B cells. *Proc. Natl. Acad. Sci. USA.* 2006; 103:395–400. [PubMed: 16387847]

19. Vuong BQ, et al. Specific recruitment of protein kinase A to the immunoglobulin locus regulates class-switch recombination. *Nat. Immunol.* 2009; 10:420–426. [PubMed: 19234474]
20. Chaudhuri J, Khuong C, Alt FW. Replication protein A interacts with AID to promote deamination of somatic hypermutation targets. *Nature.* 2004; 430:992–998. [PubMed: 15273694]
21. Yamane A, et al. Deep-sequencing identification of the genomic targets of the cytidine deaminase AID and its cofactor RPA in B lymphocytes. *Nat. Immunol.* 2011; 12:62–69. [PubMed: 21113164]
22. Yamane A, et al. RPA accumulation during class switch recombination represents 5′-3′ DNA-end resection during the S-G2/M phase of the cell cycle. *Cell Rep.* 2013; 3:138–147. [PubMed: 23291097]
23. Wold MS. Replication protein A: a heterotrimeric, single-stranded DNA-binding protein required for eukaryotic DNA metabolism. *Annu. Rev. Biochem.* 1997; 66:61–92. [PubMed: 9242902]
24. Chaudhuri J, et al. Transcription-targeted DNA deamination by the AID antibody diversification enzyme. *Nature.* 2003; 422:726–730. [PubMed: 12692563]
25. Papavasiliou FN, Schatz DG. The activation-induced deaminase functions in a postcleavage step of the somatic hypermutation process. *J. Exp. Med.* 2002; 195:1193–1198. [PubMed: 11994424]
26. Schrader CE, Guikema JE, Linehan EK, Selsing E, Stavnezer J. Activation-induced cytidine deaminase-dependent DNA breaks in class switch recombination occur during G1 phase of the cell cycle and depend upon mismatch repair. *J. Immunol.* 2007; 179:6064–6071. [PubMed: 17947680]
27. Schrader CE, Linehan EK, Mochegova SN, Woodland RT, Stavnezer J. Inducible DNA breaks in Ig S regions are dependent on AID and UNG. *J. Exp. Med.* 2005; 202:561–568. [PubMed: 16103411]
28. Maul RW, et al. Uracil residues dependent on the deaminase AID in immunoglobulin gene variable and switch regions. *Nat. Immunol.* 2011; 12:70–76. [PubMed: 21151102]
29. Imai K, et al. Human uracil-DNA glycosylase deficiency associated with profoundly impaired immunoglobulin class-switch recombination. *Nat. Immunol.* 2003; 4:1023–1028. [PubMed: 12958596]
30. Xanthoudakis S, Smeyne RJ, Wallace JD, Curran T. The redox/DNA repair protein, Ref-1, is essential for early embryonic development in mice. *Proc. Natl. Acad. Sci. USA.* 1996; 93:8919–8923. [PubMed: 8799128]
31. Schrader CE, Guikema JE, Wu X, Stavnezer J. The roles of APE1, APE2, DNA polymerase beta and mismatch repair in creating S region DNA breaks during antibody class switch. *Phil. Trans. R. Soc. Lond. B.* 2009; 364:645–652. [PubMed: 19010771]
32. Rush JS, Fugmann SD, Schatz DG. Staggered AID-dependent DNA double strand breaks are the predominant DNA lesions targeted to Sm in immunoglobulin class switch recombination. *Int. Immunol.* 2004; 16:549–557. [PubMed: 15039385]
33. Hasham MG, et al. Activation-induced cytidine deaminase-initiated off-target DNA breaks are detected and resolved during S phase. *J. Immunol.* 2012; 189:2374–2382. [PubMed: 22826323]
34. Lee JH, Paull TT. Activation and regulation of ATM kinase activity in response to DNA double-strand breaks. *Oncogene.* 2007; 26:7741–7748. [PubMed: 18066086]
35. Lumsden JM, et al. Immunoglobulin class switch recombination is impaired in *Atm*-deficient mice. *J. Exp. Med.* 2004; 200:1111–1121. [PubMed: 15504820]
36. Reina-San-Martin B, Chen HT, Nussenzweig A, Nussenzweig MC. ATM is required for efficient recombination between immunoglobulin switch regions. *J. Exp. Med.* 2004; 200:1103–1110. [PubMed: 15520243]
37. Liu M, et al. Two levels of protection for the B cell genome during somatic hypermutation. *Nature.* 2008; 451:841–845. [PubMed: 18273020]
38. Ranjit S, et al. AID binds cooperatively with UNG and Msh2-Msh6 to Ig switch regions dependent upon the AID C terminus. *J. Immunol.* 2011; 187:2464–2475. [PubMed: 21804017]
39. Bensimon A, Aebersold R, Shiloh Y. Beyond ATM: the protein kinase landscape of the DNA damage response. *FEBS Lett.* 2011; 585:1625–1639. [PubMed: 21570395]
40. Searle JS, Schollaert KL, Wilkins BJ, Sanchez Y. The DNA damage checkpoint and PKA pathways converge on APC substrates and Cdc20 to regulate mitotic progression. *Nat. Cell Biol.* 2004; 6:138–145. [PubMed: 14743219]

41. Liu Y, et al. Interactions of human mismatch repair proteins MutS α and MutL α with proteins of the ATR-Chk1 pathway. *J. Biol. Chem.* 2010; 285:5974–5982. [PubMed: 20029092]
42. Franco S, et al. H2AX prevents DNA breaks from progressing to chromosome breaks and translocations. *Mol. Cell.* 2006; 21:201–214. [PubMed: 16427010]
43. Barlow C, et al. Atm-deficient mice: a paradigm of ataxia telangiectasia. *Cell.* 1996; 86:159–171. [PubMed: 8689683]
44. Guikema JE, et al. p53 represses class switch recombination to IgG2a through its antioxidant function. *J. Immunol.* 2010; 184:6177–6187. [PubMed: 20483782]
45. Erzberger JP, Barsky D, Scharer OD, Colvin ME, Wilson DM. 3rd Elements in abasic site recognition by the major human and *Escherichia coli* apurinic/apyrimidinic endonucleases. *Nucleic Acids Res.* 1998; 26:2771–2778. [PubMed: 9592167]
46. Ishiai M, Sanchez JP, Amin AA, Murakami Y, Hurwitz J. Purification, gene cloning, and reconstitution of the heterotrimeric single-stranded DNA-binding protein from *Schizosaccharomyces pombe*. *J. Biol. Chem.* 1996; 271:20868–20878. [PubMed: 8702843]

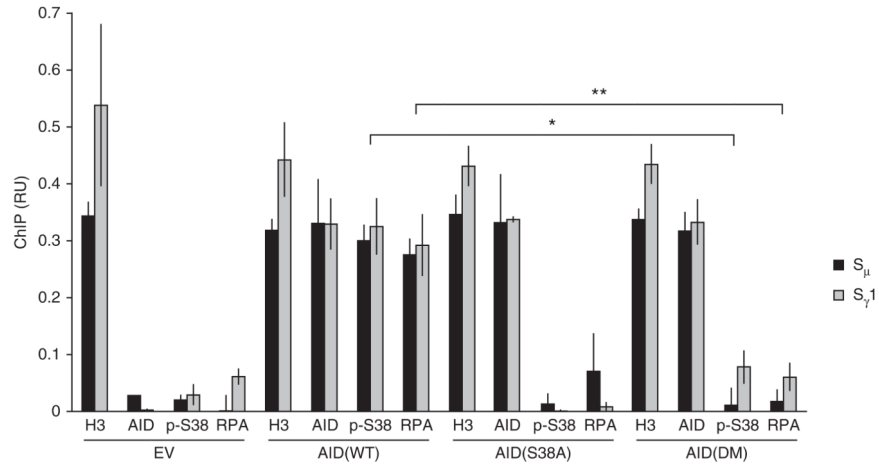


Figure 1.

Catalytically inactive AID bound to S regions is not efficiently phosphorylated. ChIP and quantitative PCR analysis of *Aicda*^{-/-} B cells retrovirally infected to express empty vector (EV) or vector encoding AID(WT), AID(S38A) or AID(DM) and stimulated for 3 d with LPS plus IL-4, assessing the abundance of histone H3, AID, p-Ser38–AID or RPA (horizontal axis) at S_μ or S_{γ1} (key), presented as relative units (RU) calculated as follows: normalization of the cycling threshold (Ct) of DNA obtained by ChIP with a specific antibody to that of input DNA, followed by calculation of the inverse of that normalized Ct and subtraction of the ‘IgG preclear’ value (inverse of the normalized Ct for ChIP with IgG) from the value obtained for the ChIP with a specific antibody (inverse of the normalized Ct). **P* < 0.01 and ***P* < 0.008, results for p-Ser38–AID or RPA in cells expressing AID(WT) versus those in cells expressing AID(DM) (paired, two-tailed Student’s *t*-test). Data represent three independent experiments (mean and s.d.).

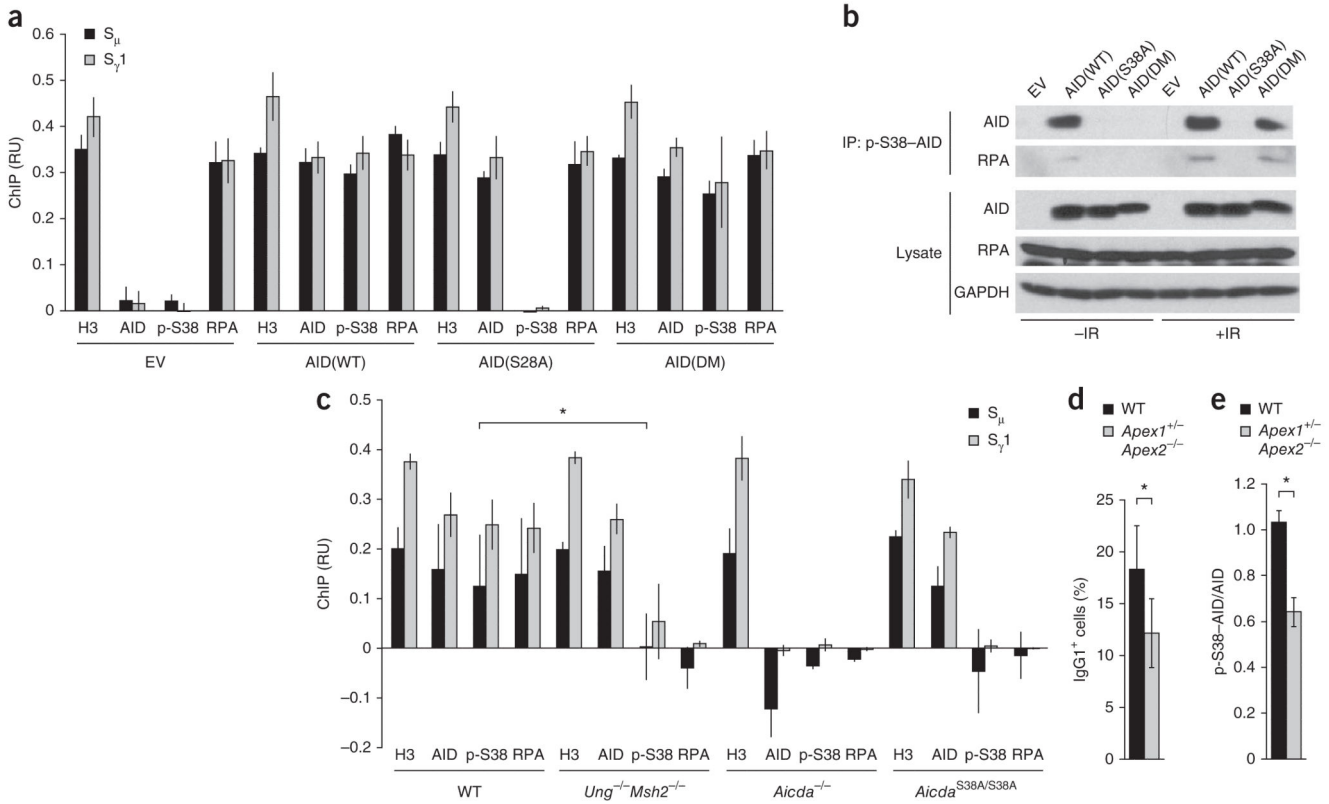


Figure 2.

Phosphorylation of AID at Ser38 is induced by DNA breaks. **(a)** ChIP and quantitative PCR analysis (as in Fig. 1) of *Aicda*^{-/-} B cells infected and stimulated as in Figure 1 and treated with ionizing radiation (10 Gy). **(b)** Immunoassay of *Aicda*^{-/-} B cells retrovirally infected to express empty vector or various forms of AID (above lanes) and left untreated (-IR) or treated (+IR) with ionizing radiation (10 Gy), assessed by immunoprecipitation (IP) with antibody to p-Ser38-AID covalently conjugated to agarose beads followed by immunoblot analysis of immunoprecipitates (top two) and lysates (bottom three) with anti-AID, anti-RPA or anti-GAPDH (loading control throughout). **(c)** ChIP and quantitative PCR analysis (as in Fig. 1) of naive wild-type BALB/c (WT), *Ung*^{-/-}*Msh2*^{-/-}, *Aicda*^{-/-} or *Aicda*^{S38A/S38A} splenic B cells stimulated for 48 h *ex vivo* with LPS plus IL-4. **P* < 0.03, wild-type versus *Ung*^{-/-}*Msh2*^{-/-} (paired, two-tailed Student's *t*-test). **(d)** Frequency of cells expressing surface IgG1 among naive wild-type or *Apex1*^{+/-}*Apex2*^{-/-} splenic B cells stimulated for 96 h *ex vivo* with LPS plus IL-4, analyzed by flow cytometry. **P* < 0.04, wild-type versus *Apex1*^{+/-}*Apex2*^{-/-} (paired, two-tailed Student's *t*-test). **(e)** ChIP analysis of wild-type and *Apex1*^{+/-}*Apex2*^{-/-} B cells stimulated as in **c**, presented as the ratio of the abundance of p-Ser38-AID at S_{γ1} to that of AID at S_{γ1}. **P* < 0.001 (paired, two-tailed Student's *t*-test). Data represent three independent experiments (**a,c-e**; mean and s.d.) or are representative of four independent experiments (**b**).

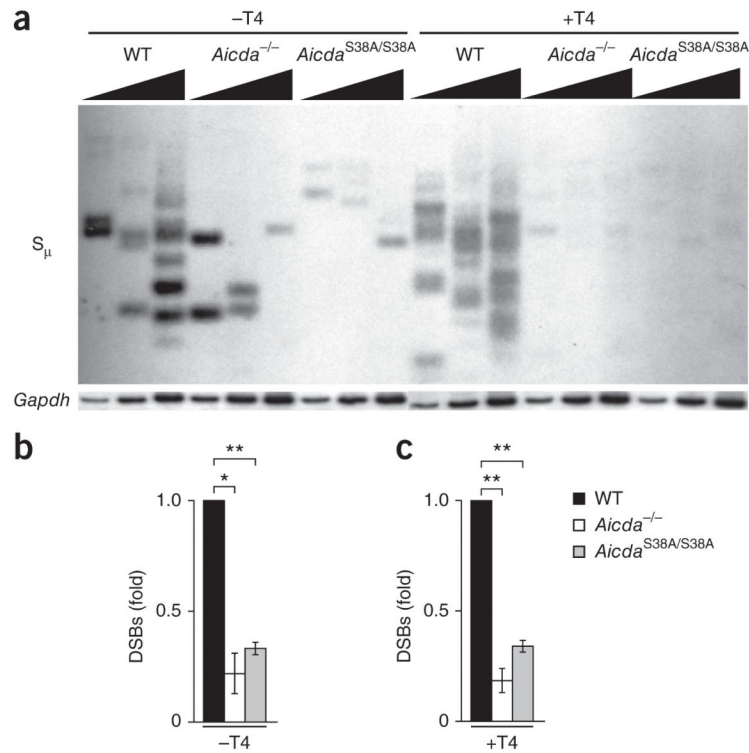


Figure 3.

Aicda^{S38A/S38A} B cells have fewer DSBs. **(a)** LM-PCR analysis of DNA from naive wild-type BALB/c, *Aicda*^{-/-} or *Aicda*^{S38A/S38A} splenic B cells stimulated *ex vivo* with LPS plus IL-4 and left untreated (-T4) or treated (+T4) with T4 DNA polymerase, assessed with primers specific for S_μ or by amplification of *Gapdh* (internal control for template loading⁴²).

Wedges indicate a threefold increase in DNA. **(b,c)** LM-PCR analysis of DSBs in S_μ of wild-type BALB/c, *Aicda*^{-/-} or *Aicda*^{S38A/S38A} B cells stimulated with LPS alone (for analysis of CSR to IgG3; autoradiographs, Supplementary Fig. 6), LPS plus IL-4 (for analysis of CSR to IgG1), or LPS plus interferon-γ (for analysis of CSR to IgG2a), in the absence **(b)** or presence **(c)** of T4 DNA polymerase, quantified by compilation of densitometry results for autoradiographs and presented relative to the results of wild-type cells. **P* < 0.001 and ***P* < 0.0001 (paired, two-tailed Student's *t*-test). Data are representative of three experiments **(a)** or represent three independent experiments **(b,c)**; mean and s.d.).

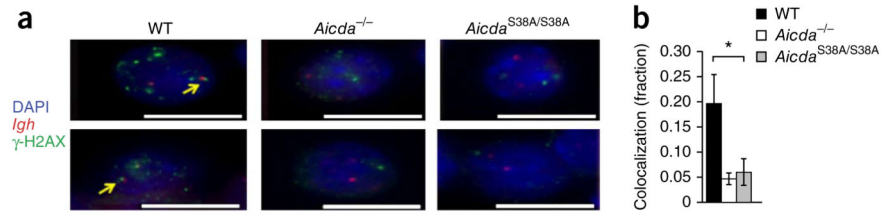


Figure 4.

Aicda^{S38A/S38A} B cells have less colocalization of *Igh* with γ -H2AX foci. (a) Wide-field images of immuno-FISH of naive wild-type BALB/c, *Aicda*^{-/-} or *Aicda*^{S38A/S38A} splenic B cells stimulated *ex vivo* with anti-CD40 plus IL-4, assessed with a bacterial artificial chromosome probe for *Igh* (red) and antibody to γ -H2AX (green) and by staining of DNA with the DNA-intercalating dye DAPI (blue); yellow arrows indicate colocalization of *Igh* and γ -H2AX. Scale bars, 10 μ m. (b) Frequency of wild-type BALB/c, *Aicda*^{-/-} or *Aicda*^{S38A/S38A} B cells ($n = 100$ per genotype per experiment) with colocalization of at least one *Igh* signal and γ -H2AX focus (as in a; actual cell numbers, Supplementary Fig. 7). * $P < 0.04$ (paired, two-tailed Student's *t*-test). Data are representative of three independent experiments (mean and s.d. in b)

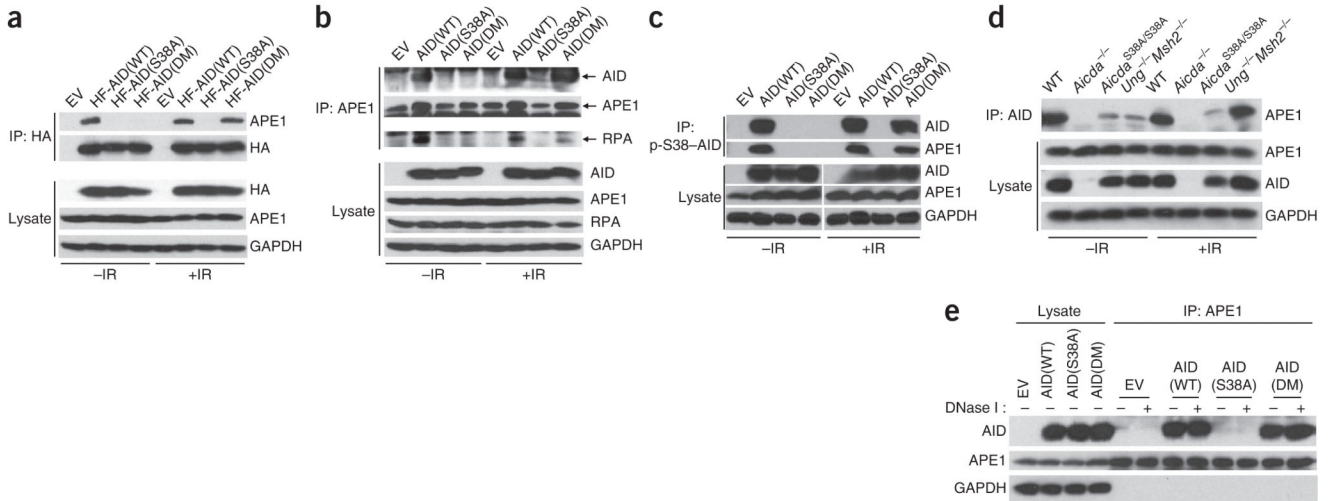


Figure 5.

AID interacts with APE1. **(a)** Immunoassay of *Aicda*^{-/-} B cells infected to express empty vector or HA-Flag-tagged (HF-) AID(WT), AID(S38A) or AID(DM), stimulated with LPS plus IL-4 and left untreated or treated with ionizing radiation (10 Gy), assessed by immunoprecipitation of proteins from NP-40 lysates with anti-HA covalently conjugated to agarose beads followed by immunoblot analysis of immunoprecipitates (top two) and lysates (bottom three) with anti-HA, anti-APE1 or anti-GAPDH. **(b)** Immunoassay of *Aicda*^{-/-} B cells infected to express empty vector or untagged AID(WT), AID(S38A) or AID(DM) and stimulated and treated as in **a**, assessed by immunoprecipitation of proteins from NP-40 lysates with anti-APE1 followed by immunoblot analysis of immunoprecipitates and lysates with anti-AID, anti-APE1, anti-RPA or anti-GAPDH. The immunoglobulin light chain migrates very close to AID, and the two polypeptides are often difficult to resolve by immunoblot analysis. **(c)** Immunoassay of *Aicda*^{-/-} B cells infected, stimulated and treated as in **b**, assessed by immunoprecipitation of proteins from NP-40 lysates with antibody to p-Ser38-AID covalently conjugated to agarose beads followed by immunoblot analysis of immunoprecipitates and lysates with anti-AID, anti-APE1 or anti-GAPDH. **(d)** Immunoassay of naive wild-type, *Aicda*^{-/-}, *Aicda*^{S38A/S38A} or *Ung*^{-/-}*Msh2*^{-/-} splenic B cells stimulated for 72 h *ex vivo* with LPS plus IL-4 and left untreated or treated with ionizing radiation (10 Gy), assessed by immunoprecipitation of proteins from NP-40 lysates with anti-AID followed by immunoblot analysis of immunoprecipitates with anti-APE1 and of lysates with anti-APE1, anti-AID or anti-GAPDH. **(e)** Immunoassay of *Aicda*^{-/-} splenic B cells infected as in **b** and treated with 10 Gy ionizing radiation, followed by treatment of NP-40 lysates for 30 min at 25 °C with DNase I (+) or no DNase I (-) and immunoprecipitation with anti-APE1 and subsequent immunoblot analysis of immunoprecipitates and lysates with anti-AID, anti-APE1 or anti-GAPDH. Data are representative of three (**a-c**) or two (**d,e**) independent experiments.

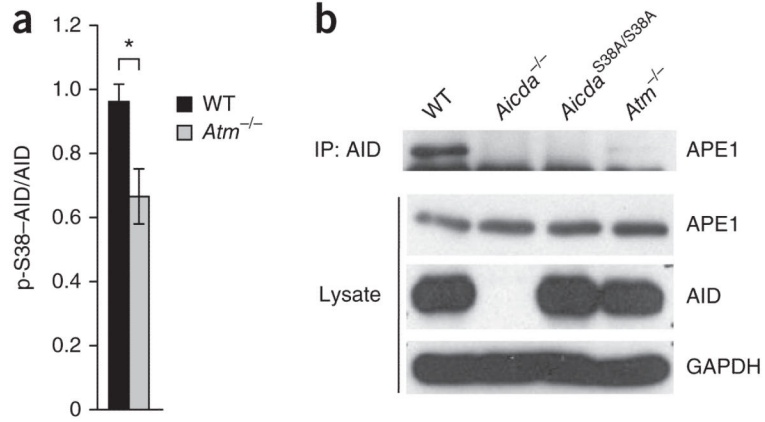


Figure 6.

ATM is required for the phosphorylation of AID bound to S regions and the interaction of AID with APE1. **(a)** ChIP analysis of naive wild-type BALB/c or *Atm*^{-/-} splenic B cells stimulated for 48 h *ex vivo* with LPS plus IL-4, presented as the ratio of the abundance of p-Ser38-AID at S_γ1 to that of AID at S_γ1. **P* < 0.007 (paired, two-tailed Student's *t*-test). **(b)** Immunoassay of naive wild-type BALB/c, *Aicda*^{-/-}, *Aicda*^{S38A/S38A} or *Atm*^{-/-} splenic B cells stimulated for 72 h *ex vivo* with LPS plus IL-4, assessed by immunoprecipitation of proteins from NP-40 lysates with anti-AID and immunoblot analysis of immunoprecipitates and lysates with anti-APE1, anti-AID or anti-GAPDH. Data represent three independent experiments **(a)**; mean and s.d.) or are representative of three independent experiments **(b)**.